CANCER GENOMICS & PROTEOMICS *19*: 526-539 (2022)
doi:10.21873/cgp.20338

Mesonephric-like Adenocarcinoma of the Uterine Corpus: Comprehensive Analyses of Clinicopathological, Molecular, and Prognostic Characteristics With Retrospective Review of 237 Endometrial Carcinoma Cases

HAN GYEOL KIM[1,2], HYUNJIN KIM[3], MIN-KYUNG YEO[4], KYU YEOUN WON[5], YOUNG SUN KIM[6], GWAN HEE HAN[7], HYUN-SOO KIM[2] and KIYONG NA[1]

[1]Department of Pathology, Kyung Hee University Hospital, Kyung Hee University College of Medicine, Seoul, Republic of Korea;
[2]Department of Pathology and Translational Genomics, Samsung Medical Center, Sungkyunkwan University School of Medicine, Seoul, Republic of Korea;
[3]Pathology Center, Seegene Medical Foundation, Seoul, Republic of Korea;
[4]Department of Pathology, Chungnam National University School of Medicine, Daejeon, Republic of Korea;
[5]Department of Pathology, Kyung Hee University Hospital at Gangdong, Kyung Hee University College of Medicine, Seoul, Republic of Korea;
[6]Department of Obstetrics and Gynecology, Kyung Hee University Hospital, Kyung Hee University College of Medicine, Seoul, Republic of Korea;
[7]Department of Obstetrics and Gynecology, Kyung Hee University Hospital at Gangdong, Kyung Hee University College of Medicine, Seoul, Republic of Korea

Abstract. *Background/Aim: Uterine mesonephric-like adenocarcinoma (MLA) is a rare malignant tumor of the female genital tract. Patients and Methods: We reviewed 237 endometrial carcinoma cases and investigated the clinicopathological and molecular characteristics of uterine MLA. Results: We found that 3.0% (7/237) of the endometrial carcinoma cases were MLAs. Compared to endometrial endometrioid carcinoma, MLA showed larger tumor size, deeper myometrial invasion, increasingly advanced-stage disease, and more frequent lymphovascular space invasion. All MLAs exhibited architectural diversity, compactly aggregated small tubules, eosinophilic intraluminal secretions, overlapped and angulated nuclei, scant cytoplasm, and presence of spindle cells. All the MLAs expressed at least two mesonephric markers. All except one MLA harbored activating Kirsten rat sarcoma viral oncogene homolog mutations. All patients with MLA developed postoperative metastases. MLA had the lowest progression-free survival rate among different histological types of endometrial carcinoma. Conclusion: Uterine MLA is a highly aggressive gynecological malignancy, showing unique morphological and molecular features, frequent recurrences and metastases, as well as poor prognosis.*

Correspondence to: Kiyong Na, Department of Pathology, Kyung Hee University Hospital, Kyung Hee University College of Medicine, 26, Kyungheedae-ro, Dongdaemun-gu, Seoul 02447, Republic of Korea. Tel: +82 29588740, Fax: +82 29588744, e-mail: raripapa@gmail.com; Hyun-Soo Kim, Department of Pathology and Translational Genomics, Samsung Medical Center, Sungkyunkwan University School of Medicine, 81, Irwon-ro, Gangnam-gu, Seoul 06351, Republic of Korea. Tel: +82 234101243, Fax: +82 234132831, e-mail: hyun-soo.kim@samsung.com

Key Words: Uterine mesonephric-like adenocarcinoma, endometrial carcinoma, targeted sequencing, mesonephric markers.

This article is an open access article distributed under the terms and conditions of the Creative Commons Attribution (CC BY-NC-ND) 4.0 international license (https://creativecommons.org/licenses/by-nc-nd/4.0).

Mesonephric adenocarcinoma (MA) is a rare malignant tumor of the female genital tract. It is thought to originate from the mesonephric remnants (1-3), which are usually located in the lateral wall of the vagina and uterine cervix, the broad ligament, and the ovarian hilum (4, 5). The term mesonephric-like adenocarcinoma (MLA) has been suggested for a malignant tumor arising in the uterine corpus and the adnexa. MLA shows similar histological, immunophenotypical, and genetic features to those of cervical MA (1, 6-12). It is morphologically characterized by various architectural patterns, such as tubular, ductal, papillary, spindle, solid, trabecular, retiform, and sex cord-like (1, 6, 8, 9). Diverse growth patterns make it difficult

to distinguish uterine MLA from more commonly encountered histological types of endometrial carcinoma, including endometrial endometrioid carcinoma (EC) (10), serous carcinoma (SC), and carcinosarcoma (CS). A unique immunophenotype of MLA has also been documented in the literature (2, 6, 13, 14). The following expression patterns support the diagnosis of MLA: positive immunoreactivities for mesonephric markers, including GATA-binding protein 3 (GATA3), paired box 2 (PAX2), transcription termination factor 1 (TTF1), and cluster of differentiation 10 (CD10); negative or only focal expression of hormone receptors; non-diffuse p16 positivity; and wild-type p53 immunostaining pattern (1, 2, 5, 6, 8, 9). Molecular studies using targeted next-generation sequencing (NGS) revealed that patients with uterine MLA frequently harbor a pathogenic mutation in the Kirsten rat sarcoma viral oncogene homolog (*KRAS*) gene, as well as alterations in neuroblastoma viral oncogene homolog, AT-rich interaction domain (*ARID1A*), phosphatidylinositol-4,5-bisphosphate 3-kinase catalytic subunit alpha (*PIK3CA*), β-catenin, patched 2, and tumor protein 53 (*TP53*) (1, 8, 9, 15).

It has been consistently reported in several case series that distant metastases and late recurrences frequently occur in patients with uterine MLA (1, 9). Advanced International Federation of Gynecology and Obstetrics (FIGO) stage at the time of initial diagnosis and rapid disease progression despite surgery and postoperative adjuvant therapy may explain the dismal prognosis of uterine MLA (9). To date, less than 200 cases of MLA arising in the uterine corpus have been reported in the literature (1, 2, 9, 11). Most of these previous publications are relatively small case series or individual case reports. Uterine MLA is a rare but important and distinct condition, and its clinicopathological and molecular characteristics should be clarified. In this study, we aimed to identify uterine MLA cases retrospectively and estimate the prevalence of this rare tumor through a slide review of consecutive endometrial carcinoma cases in two institutions. Then, we analyzed their clinical, histological, immunophenotypical, and molecular characteristics using immunostaining and NGS. Further, the detailed histological features of uterine MLA were compared with those of other endometrial carcinoma types. Our observations on uterine MLA should allow pathologists to recognize and accurately diagnose this condition.

Patients and Methods

Case selection and clinicopathological data collection. This study protocol (2020-03-065) was reviewed and approved by the Institutional Review Board of Kyung Hee University Hospital. We searched the data on 237 consecutive cases of endometrial carcinoma in the surgical pathology databases of Kyung Hee University Hospital (148 cases; from January 2003 to October 2019) and Kyung Hee University Hospital at Gangdong (89 cases; from January 2013 to March 2020). The following clinical information was obtained from the electronic medical records: age of patient at diagnosis, serum cancer antigen (CA) 125 level, initial FIGO stage, nodal metastasis, development of recurrence and/or metastasis, progression-free survival (PFS), tumor size, invasion depth, and lymphovascular space invasion (LVSI). Two board-certified gynecological pathologists reviewed all the available hematoxylin and eosin-stained slides by using light microscopy. The following pathological information was determined after slide review: tumor border, nuclear pleomorphism, chromatin pattern, nuclear overlapping and angulation, amount of cytoplasm, number of architectural patterns, presence of eosinophilic intraluminal secretions, squamous or mucinous differentiation, spindle cells, coagulative tumor cell necrosis, and mitotic count per 10 high-power fields (HPFs). The most representative slide was selected for performing immunostaining and NGS.

Immunohistochemical staining. Four-micrometer-thick, formalin-fixed, paraffin-embedded (FFPE) slices were deparaffinized and rehydrated using a xylene and alcohol solution. Immunostaining was performed using an automated instrument (Leica Biosystems, Buffalo Grove, IL, USA) (1, 2, 5, 16-27). After antigen retrieval, the FFPE slices were incubated with primary antibodies against GATA3 (1:200, clone L50-823, Cell Marque, Rocklin, CA, USA), PAX2 (1:200, clone EP3251, Abcam, Cambridge, UK), CD10 (1:50, clone NCL-L-CD10-270, Novocastra, Leica Biosystems, Vista, CA, USA), TTF1 (1:1,000, clone 8G7G3/1, Dako, Agilent Technologies, Santa Clara, CA, USA), estrogen receptor (ER; 1:200, clone NCL-L-ER-6F11, Novocastra), progesterone receptor (PR; 1:200, clone PGR-312-L-CE, Novocastra), p16 (prediluted, clone E6H4, Ventana Medical Systems, Roche, AZ, USA), and p53 (1:200, clone DO-7, Dako). After chromogenic visualization, the slices were counterstained with hematoxylin. Appropriate positive and negative controls were concurrently stained to validate the staining method. Invasive breast carcinoma of no specific type, normal thyroid tissue, normal proliferative-phase endometrium, and ovarian high-grade serous carcinoma were used as positive controls for GATA3; TTF1; PAX2, CD10, ER, and PR; and p53 and p16, respectively. Negative controls were prepared by substituting non-immune serum for primary antibodies, resulting in no detectable staining.

Immunohistochemical interpretation. The intensity of positive staining was graded as strong, moderate, and weak. The proportion of positive staining was established as diffuse when 50% or more of the tumor cells were stained, patchy when 5-49% were stained, and focal when less than 5% were stained. For PAX2, GATA3, ER, PR, and TTF1, staining in the nuclei was interpreted as positive expression (1). For CD10, we examined the subcellular localization of positive immunoreactivity. In particular, CD10 immunoreactivity along the luminal surfaces of neoplastic tubules and ducts was considered as positive expression, supporting the diagnosis of MLA (2, 5). p53 expression was interpreted as having a mutated pattern when one of the following staining patterns was observed: diffuse and strong nuclear immunoreactivity in ≥75% of the tumor cells (over-expression pattern); no nuclear immunoreactivity in any of the tumor cells (complete absence pattern); or an unequivocal cytoplasmic staining accompanied by variable nuclear staining (cytoplasmic pattern) (28). In contrast, p53 expression was interpreted as wild-type if variable proportions of tumor cell nuclei were stained with mild-to-moderate intensity (17, 19, 29, 30). p16 expression was interpreted as diffuse and strong when it was continuous and intense, with nuclear or nuclear plus cytoplasmic

Table I. *Clinicopathological characteristics of uterine mesonephric-like adenocarcinoma (MLA).*

Case No.	Age (years)	Initial stage	Invasion depth	LVSI	Initial LN metastasis	Initial adnexal metastasis	Initial peritoneal metastasis	Initial distant metastasis	Eosinophilic intraluminal secretion	Architectural pattern	CTCN	Postoperative recurrence	PFS (months)
1	62	IIIA	DM	+	–	+	–	–	+	Tubular, ductal, cribriform, papillary, solid, spindle, glomeruloid	–	+ (liver, peritoneum)	6
2	72	IB	DM	+	–	–	–	–	+	Tubular, papillary, solid, trabecular	+	+ (lungs, PALN, vaginal stump)	8
3	62	IIIC	PM, serosa	+	+ (pelvic)	–	+ (pelvic peritoneum)	–	+	Tubular, ductal, papillary, solid, glomeruloid, retiform, trabecular	–	+ (lungs, pleura, peritoneum, pancreas, spleen)	8
4	63	IB	DM	+	–	–	–	–	+	Tubular, ductal, cribriform, papillary, retiform	+	+ (lungs, PALN)	4
5	59	IIIA	Serosa	+	–	–	–	–	+	Tubular, ductal, cribriform, solid, retiform	+	+ (peritoneum)	89
6	69	IB	DM	+	–	–	–	–	+	Tubular, ductal, papillary, retiform	–	+ (lungs)	14
7	66	IVB	PM, serosa	+	+ (para-aortic)	–	–	+ (lungs)	+	Tubular, ductal, cribriform, papillary, solid, spindle	–	NA (due to follow-up loss)	NA

CTCN: Coagulative tumor cell necrosis; DM: deep myometrium; LVSI: lymphovascular space invasion; NA: not applicable; PFS: progression-free survival; PALN: para-aortic lymph node; PM: parametrium.

staining. All other p16 immunostaining patterns, described as focal nuclear staining or wispy, blob-like, puddled, or scattered cytoplasmic staining, were interpreted as patchy (1, 17, 29-31).

NGS. Five-micrometer-thick FFPE tissue slides were deparaffinized and hydrated using a series of graded alcohols and finally water. The slides were manually microdissected using a scalpel dipped in ethanol. The scraped material was washed in phosphate-buffered saline and digested using proteinase K and buffer ATL (Qiagen, Hilden, Germany) overnight at 56˚C. DNA and RNA were then isolated using a QIAamp DSP DNA FFPE Tissue Kit (Qiagen) according to the manufacturer's instructions (2, 18, 32). A Qubit 4 Fluorometer (Thermo Fisher Scientific, Waltham, MA, USA) was used to quantify the extracted samples of nucleic acids using highly sensitive and accurate fluorescence-based quantitation assays. Furthermore, NGS libraries were prepared using the samples and Ion AmpliSeq Library Preparation on the IonChef System according to protocol (Thermo Fisher Scientific). Sequencing was performed on the IonTorrent S5 XL platform, using positive control cell line mixtures (Horizon Discovery, Cambridge, UK) and the Oncomine Comprehensive Assay v3 (Thermo Fisher Scientific), an amplicon-based, targeted assay that enables the detection of relevant single-nucleotide variants, amplifications, and indels from 161 unique genes. Genomic data were analyzed and alterations in the genome were detected using the IonReporter software v5.6 (Thermo Fisher Scientific). We also reviewed the variant call format file using the Integrated Genomic Viewer. Only variants in coding regions, promoter regions, or splicing sites were retained. The criteria for identifying mutant alleles were as follows: minimum depth of coverage, 500×; mutant allele frequency, >5%; and exclusion of silent and nonexonic variants.

Statistical analysis. Mann–Whitney test, chi-square test, or Fisher's exact test was used to examine the differences among variants. Univariate survival analysis was performed to examine the prognostic significance with respect to PFS. Kaplan–Meier curves were constructed and compared using the log rank test. All statistical analyses were performed using IBM SPSS Statistics for Windows, version 23.0 (IBM Corp., Armonk, NY, USA). Statistical significance was defined as $p<0.05$.

Results

Clinicopathological characteristics of uterine MLA (Table I). Among the 237 consecutive endometrial carcinoma cases, seven (3.0%) were of uterine MLA. Age at diagnosis ranged from 59 to 72 years (mean, 63 years). Serum CA 125 levels were elevated in three patients (53.98, 67.86, and 50.8 U/ml, respectively). In five of the seven cases, endometrial curettage specimens were not diagnosed as MLA but as one of the following: grade 2 EC (2/5), grade 3 EC (1/5), SC (1/5), and mixed EC and CCC (1/5). All patients underwent total hysterectomy with bilateral salpingo-oophorectomy, pelvic or para-aortic lymph node dissection, or peritonectomy. Mean tumor size was 5.2 cm (range=4.0-7.0 cm). All tumors invaded the deep myometrium. Three of them penetrated the serosa, of which two extended into the parametrium. LVSI was identified in all cases. Three patients had synchronous metastases in the

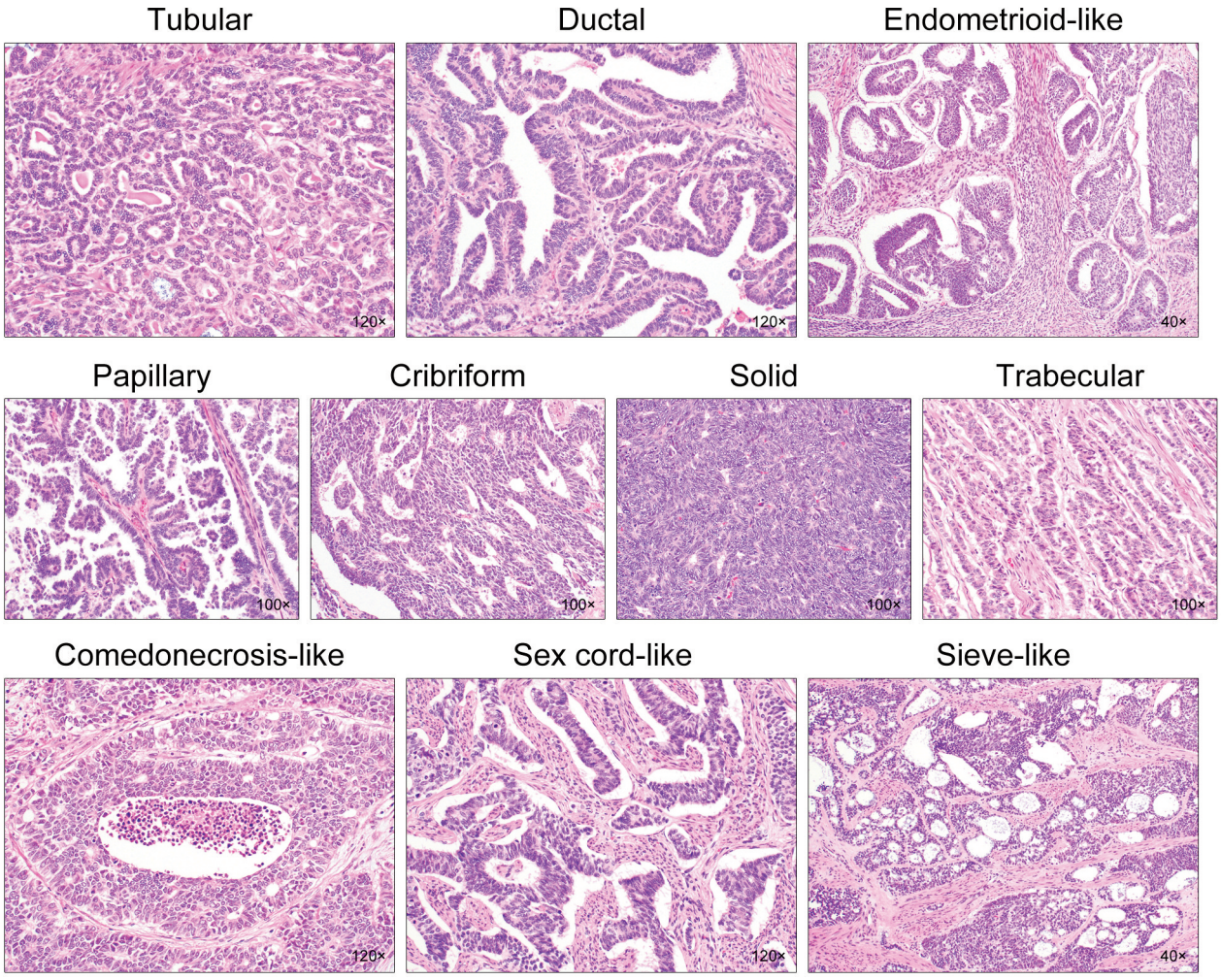


Figure 1. *Architectural diversity of uterine mesonephric-like adenocarcinoma (MLA). All MLA cases displayed compact aggregation of small tubules lined by cuboidal-to-low columnar epithelial cells and possessed eosinophilic intraluminal secretions (tubular pattern). Ductal, glandular, cribriform, and solid growth patterns resembling those of endometrioid carcinoma were observed in most cases. Numerous papillae with delicate fibrovascular stromal cores in MLA were similar to those of serous carcinoma. Trabecular and sex cord-like architecture resembled that of sertoliform endometrioid carcinoma. Unusual growth patterns, including comedonecrosis-like and sieve-like patterns, were occasionally noted in uterine MLA.*

adnexa, pelvic and para-aortic lymph nodes, pelvic peritoneum, and lungs. The initial FIGO stages were distributed as follows: stage IB (3/7), IIIA (2/7), IIIC (1/7), and IVB (1/7). Postoperative follow-up information was available for six patients, while the remaining patient was referred to another hospital after surgery. All six patients developed postoperative recurrences in the lungs, liver, pancreas, spleen, para-aortic lymph nodes, peritoneum, and vaginal stump. The lung was the most common site of metastasis (5/7). Median PFS of patients with uterine MLA was 8 months.

Histologically, uterine MLA showed various architectural patterns (Figure 1), including tubular, ductal, endometrioid-like, papillary, cribriform, solid, trabecular, comedonecrosis-like, sex cord-like, sieve-like, retiform, and glomeruloid. All cases showed relatively small, overlapped, angulated nuclei with grooves, low-to-intermediate degree of nuclear atypia, scant cytoplasm, and high nuclear-to-cytoplasmic ratio. Only one case showed a few microscopic foci of severe nuclear pleomorphism and conspicuous nucleoli. Eosinophilic, hyaline-like intraluminal secretions were noted within the tubules and glands of all cases. These also looked similar to the colloid observed in the thyroid follicles. The secretions were usually observed to have a dense form; however, they also showed a pale, granular form or the presence of a small number of cells. These forms could be distinguished from the intraluminal necroses, showing an admixture of fibrin, karyorrhectic debris, ghost-like tumor cells, and extravasated red blood cells. We also noted some irregular-shaped sheets

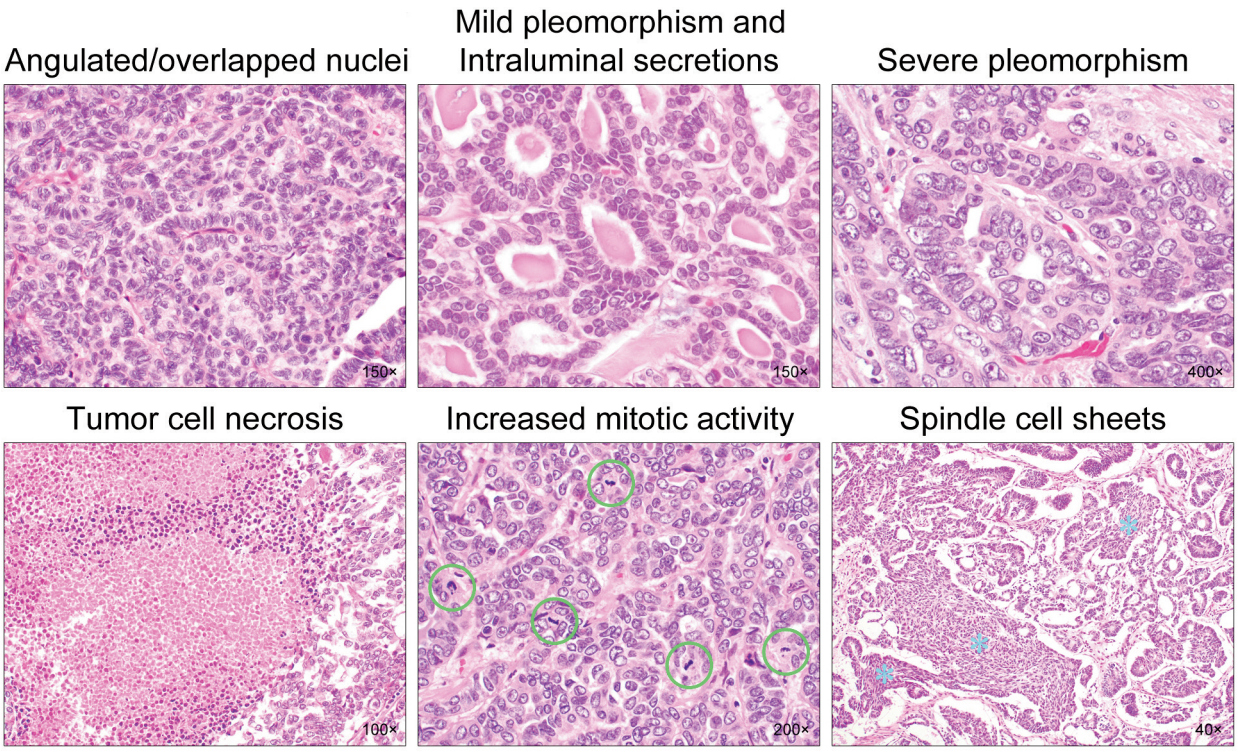


Figure 2. *Typical and atypical histological features of uterine MLA. All MLA cases exhibited angulated and overlapping nuclei with minimal-to-mild pleomorphism. Scant cytoplasm resulted in high nuclear-to-cytoplasmic ratio. Eosinophilic intraluminal secretions, characteristic of MLA, were easily identifiable. However, some microscopic foci showed severe nuclear pleomorphism, tumor necrosis, and brisk mitotic activity (green circles). Although uterine MLA does not have areas of squamous differentiation, variable-sized sheets and nests of spindle-shaped tumor cells (blue asterisks) closely resemble squamous morules of endometrioid carcinoma.*

of spindle cells arranged in a whorled or fascicular pattern. These resembled the immature squamous morules of EC but did not show any intercellular bridges, distinct cell borders, or keratinization. Representative photomicrographs of these histological features of uterine MLA are shown in Figure 2.

Immunophenotypes of uterine MLA (Table II). All except one case exhibited moderate-to-strong nuclear immunoreactivity for GATA3. Tumors in five of the seven cases were moderately positive for TTF1. Consistent with previous data (2, 14), we found one case displaying an inverse pattern of GATA3 and TTF1 staining. Microscopic tumor areas that were strongly positive for GATA3 were completely negative for TTF1. All tumors diffusely expressed PAX2 in at least 50% of the tumor cells. CD10 was also expressed in all except one case, with at least moderate staining intensity. Taken together, all cases demonstrated positive immunoreactivities for at least two of the four mesonephric markers. There was no significant difference in the degree of nuclear atypia or the proportion of growth pattern by the protein expression status. Tumors in six cases were completely negative for ER, while that in the remaining one displayed scattered microscopic foci of weak-to-moderate ER staining, occupying 10% of the entire tumor area. The tumor cells expressing ER were not morphologically different from the ER-negative ones. All cases showed negative PR immunoreactivity, patchy p16 expression, and wild-type p53 immunostaining pattern. Representative photomicrographs of immunophenotypes of uterine MLA are shown in Figure 3.

NGS results of uterine MLA (Table III). Targeted sequencing analyses were performed in all except one case, of which the tumor tissue was unavailable for NGS. We observed that all examined uterine MLAs (6/6) harbored pathogenic *KRAS* mutations, including p.G12D (3/6), p.G12V (2/6), and p.G12C (1/6). Three cases had additional pathogenic truncating mutations in *ARID1A* (2/6; p.Q1650* and p.Q723fs) and ataxia telangiectasia mutated (*ATM*; 1/6; p.F2799fs).

Clinical characteristics of other histological types of endometrial carcinoma. We identified 194, 16, and 20 cases of EC, SC, and CS, respectively. Mean age of the 194 EC patients at time of diagnosis was 55.9 years (range=32-82 years). They were classified according to FIGO stages as follows: stage 1 (93/194), 2 (54/194), and 3 (47/194).

Table II. *Immunophenotypes of uterine mesonephric-like adenocarcinoma (MLA).*

Case No.	GATA3 (nuclear)		CD10 (luminal)		TTF1 (nuclear)		PAX2 (nuclear)		ER (nuclear)		PR (nuclear)	
	Intensity	Proportion (pattern)	Intensity	Proportion (pattern)	Intensity	Proportion (pattern)	Intensity	Proportion (pattern)	Intensity	Proportion (pattern)	Intensity	Proportion (pattern)
1	Moderate	30% (patchy)	Moderate	1% (focal)	Strong	10% (patchy)	Strong	80% (diffuse)	Absent	0% (–)	Absent	0% (–)
2	Strong	25% (patchy)	Strong	20% (patchy)	Absent	0% (–)	Strong	60% (diffuse)	Absent	0% (–)	Absent	0% (–)
3	Strong	10% (patchy)	Strong	95% (diffuse)	Strong	90% (diffuse)	Strong	85% (diffuse)	Absent	0% (–)	Absent	0% (–)
4	Moderate	1% (focal)	Absent	0% (–)	Moderate	20% (patchy)	Weak	50% (diffuse)	Moderate	10% (patchy)	Absent	0% (–)
5	Absent	0% (–)	Strong	70% (diffuse)	Absent	0% (–)	Strong	70% (diffuse)	Absent	0% (–)	Absent	0% (–)
6	Strong	80% (diffuse)	Strong	5% (patchy)	Strong	70% (diffuse)	Strong	99% (diffuse)	Absent	0% (–)	Absent	0% (–)
7	Moderate	30% (patchy)	Strong	25% (patchy)	Moderate	1% (focal)	Strong	60% (diffuse)	Absent	0% (–)	Absent	0% (–)

ER: Estrogen receptor; GATA3: GATA-binding protein 3; PAX2: paired box 2; PR: progesterone receptor; TTF1: transcription termination factor 1.

Nineteen (9.8%) and six (3.1%) patients were initially diagnosed with FIGO stage III and IV ECs, respectively. Median PFS of 15 EC patients who developed postoperative recurrences was 18 months. Ages of the 16 patients with SC ranged between 46-77 years at the time of diagnosis (mean, 65.1 years). Ten (62.5%) patients had FIGO stage III-IV SCs. Eleven (55.0%) patients experienced metastatic recurrences. Median PFS of patients with recurrent SC was 10 months. The mean age of the 20 CS patients was 61.6 years (range=25-86 years). FIGO stage III-IV CSs were observed in 10 (50.0%) cases. Seven (35.0%) patients developed recurrences within 21 months after surgery.

Differences in clinicopathological features among histological types (Table IV). Statistical analyses were performed to investigate whether the clinicopathological features of uterine MLA were significantly different from those of other endometrial carcinoma types. MLA patients (mean age, 63 years) were significantly older than EC patients (mean age, 55.9 years; $p=0.004$). MLA tumors (mean tumor size, 5.2 cm) were significantly larger than those of EC (3.3 cm; $p=0.008$). All MLAs extended in more than half of the myometrium, whereas only about a quarter (49/194, 25.3%) of ECs extended into the deep myometrium ($p<0.001$). LVSI was more frequently detected in MLA (7/7, 100.0%) than EC (48/194, 24.7%; $p<0.001$) and CS (9/20, 45.0%; $p=0.022$). As shown in Table V, we compared the histological features of uterine MLA with those of EC, SC, and CS. MLA exhibited nuclear angulation and irregular nuclear membrane more frequently than EC ($p=0.002$). Both SC and CS showed severe nuclear pleomorphism more than that in MLA ($p=0.001$ and $p=0.010$, respectively). Prominent nucleoli were observed more frequently in EC, SC, and CS than in MLA ($p=0.001$, $p<0.001$, and $p<0.001$, respectively). MLA showed more scant cytoplasm than EC, SC, and CS ($p<0.001$, $p=0.044$, and $p=0.007$, respectively). MLA exhibited more frequent production of eosinophilic intraluminal secretions than that in EC, SC, and CS ($p<0.001$, $p=0.003$, and $p=0.001$, respectively). Coagulative tumor cell necrosis was more frequent in MLA than in EC ($p=0.004$). MLA had a significantly higher mean mitotic index of 18.4/10 HPFs (range=7-43/10 HPFs) than that of EC (mean 11.1/10 HPFs; $p<0.001$), while SC displayed significantly higher mitotic activity (mean, 41.3/10 HPFs) than MLA ($p=0.003$). Four or more architectural patterns were noted in all (7/7, 100.0%) MLAs, six (3.4%) ECs, one (7.7%) SC, and one (12.5%) CS. The differences in the frequencies of architectural diversity between MLA and the other histological types were significant ($p<0.001$, $p<0.001$, and $p=0.001$, respectively). Similarly, the frequencies of tubular pattern were also significantly different between MLA (7/7, 100.0%) and EC (12/240, 6.8%; $p<0.001$), SC (1/16, 7.7%; $p<0.001$), and CS (1/16, 12.5%; $p=0.001$), respectively. Both squamous (sheets of tumor cells with

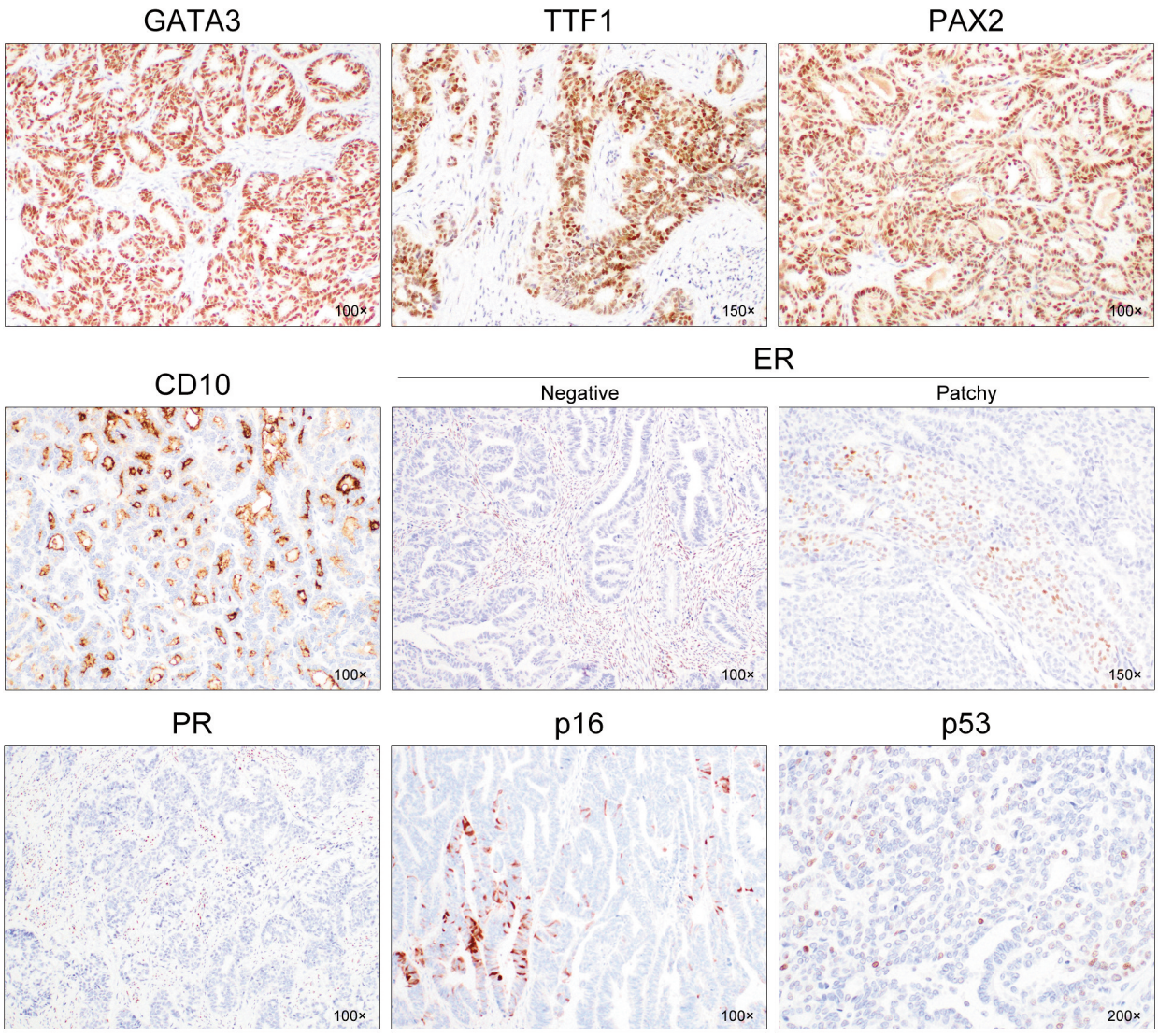


Figure 3. *Immunophenotype of uterine mesonephric-like adenocarcinoma (MLA). All cases expressed at least two of the four examined mesonephric markers, including GATA-binding protein 3 (GATA3), transcription termination factor 1 (TTF1), paired box 2 (PAX2), and cluster of differentiation (CD10). All except one case was completely negative for estrogen receptor (ER), while the one remaining tumor displayed scattered microscopic foci of weak-to-moderate ER staining. All cases showed a complete lack of progesterone receptor (PR) immunoreactivity, patchy p16 positivity, and wild-type p53 immunostaining pattern.*

intercellular bridges and distinct cell borders with or without keratinization) and mucinous differentiation (intracytoplasmic mucin) (1) were observed in EC and CS only.

Differences among the PFS of histological types (Table VI). Follow-up information was available for 233 cases (98.3%). Figure 4 depicts the Kaplan–Meier curves for the PFS of patients with EC, CS, SC, and MLA. MLA showed significantly lower PFS than that of grade 1, 2, and 3 EC ($p<0.001$, $p<0.001$, and $p<0.001$, respectively), whereas the PFS of MLA was not significantly different from that of CS and SC ($p=0.263$ and $p=0.343$, respectively). The difference between the PFS of CS and SC was not significant ($p=0.662$). Grade 3 EC showed a significantly lower PFS than that of grade 1 and 2 EC ($p<0.001$ and $p=0.012$, respectively). The difference in PFS between grade 1 and 2 EC was not significant ($p=0.207$).

Discussion

We identified 7 cases of uterine MLA out of 237 consecutive endometrial carcinoma cases. The prevalence of uterine MLA

Table III. *Pathogenic mutations of uterine mesonephric-like adenocarcinoma (MLA).*

Case No	*KRAS*			*ARID1A*			*ATM*		
	Sequence change	Amino acid change	Variant allele frequency (%)	Sequence change	Amino acid change	Variant allele frequency (%)	Sequence change	Amino acid change	Variant allele frequency (%)
1	c.35G>T	p.G12V	52.3	–	–		–	–	–
2	c.35G>A	p.G12D	73.4	–	–		–	–	–
3	c.34G>T	p.G12C	58.2	c.4948C>T	p.Q1650*	39.9	–	–	–
4	NA	NA	NA	NA	NA	NA	NA	NA	NA
5	c.35G>T	p.G12V	59.6	–	–		c.8395_8404del	p.F2799fs	49.8
6	c.35G>A	p.G12D	47.7	c.2168delA	p.Q723fs	35.2	–	–	–
7	c.35G>A	p.G12D	56.5	–	–		–	–	–

ARID1A: AR-rich domain 1A; *ATM*: ataxia telangiectasia mutated; *KRAS*: Kirsten rat sarcoma viral oncogene homolog; NA: not applicable.

Table IV. *Differences between clinical characteristics of uterine mesonephric-like adenocarcinoma (MLA) and other histological types of endometrial carcinoma.*

Characteristic	MLA	EC	*p*-Value (MLA *vs.* EC)	SC	*p*-Value (MLA *vs.* SC)	CS	*p*-Value (MLA *vs.* CS)
Mean age (range; years)	63 (59-72)	55.9 (32-82)	0.004*	65.1 (46-77)	0.884	61.6 (25-86)	0.523
Mean tumor size (range) (cm)	5.2 (4.0-7.0)	3.3 (0.1-9.0)	0.008*	3.8 (1.2-8.0)	0.068	5.0 (0.5-10.0)	0.473
Initial FIGO stage III-IV	4 (57.1%)	25 (12.9%)	0.009*	10 (62.5%)	1.000	10 (50.0%)	1.000
Deep myometrial invasion	7 (100.0%)	49 (25.3%)	<0.001*	8 (50.0%)	0.052	12 (60.0%)	0.068
Lymphovascular space invasion	7 (100.0%)	48 (24.7%)	<0.001*	8 (50.0%)	0.052	9 (45.0%)	0.022*
Nodal metastasis	2 (28.6%)	16 (8.2%)	0.122	6 (37.5%)	1.000	8 (40.0%)	0.678
Pelvic peritoneal metastasis	1 (14.3%)	8 (4.1%)	0.278	5 (31.3%)	0.621	3 (15.0%)	1.000

CS: Carcinosarcoma; EC: endometrioid carcinoma; FIGO: International Federation of Gynecology and Obstetrics; SC: serous carcinoma. *Statistically significant.

Table V. *Differences between detailed pathological characteristics of uterine mesonephric-like adenocarcinoma (MLA) and other histological types of endometrial carcinoma.*

Characteristic	MLA	EC	*p*-Value (MLA *vs.* EC)	SC	*p*-Value (MLA *vs.* SC)	CS	*p*-Value (MLA *vs.* CS)
Infiltrative tumor border	3 (42.9%)	50 (28.6%)	0.417	6 (46.2%)	1.000	5 (62.5%)	0.619
Severe nuclear pleomorphism	1 (14.3%)	51 (29.1%)	0.187	11 (84.6%)	0.001*	6 (75.0%)	0.010*
Coarse chromatin	5 (71.4%)	147 (83.5%)	0.338	13 (100%)	0.111	8 (100.0%)	0.200
Prominent nucleoli	1 (14.3%)	112 (63.6%)	0.001*	12 (92.3%)	<0.001*	8 (100.0%)	<0.001*
Overlapping nuclei	7 (100.0%)	154 (87.5%)	1.000	9 (69.2%)	0.249	6 (75.0%)	0.467
Angulated nuclei	7 (100.0%)	69 (39.7%)	0.002*	8 (66.7%)	0.245	6 (75.0%)	0.467
Scant cytoplasm	7 (100.0%)	10 (5.7%)	<0.001*	6 (46.2%)	0.044*	2 (25.0%)	0.007*
More than three architectural patterns	7 (100.0%)	6 (3.4%)	<0.001*	1 (7.7%)	<0.001*	1 (12.5%)	0.001*
Tubular pattern	7 (100.0%)	12 (6.8%)	<0.001*	1 (7.7%)	<0.001*	1 (12.5%)	0.001*
Spindle cells	4 (57.1%)	4 (2.3%)	<0.001*	0 (0.0%)	0.007*	7 (87.5%)	0.282
Eosinophilic intraluminal secretions	7 (100.0%)	32 (18.2%)	<0.001*	3 (23.1%)	0.003*	1 (12.5%)	0.001*
Squamous or mucinous differentiation	0 (0.0%)	41 (23.3%)	0.352	0 (0.0%)	NA	2 (25.0%)	0.467
Coagulative tumor cell necrosis	3 (42.9%)	7 (4.0%)	0.004*	2 (15.4%)	0.290	2 (25.0%)	0.608
Mean mitotic count/10 high-power fields (range)	18.4 (7-43)	11.1 (0-101)	<0.001*	41.3 (7-109)	0.003*	34.9 (5-103)	0.120

CS: Carcinosarcoma; EC: endometrioid carcinoma; SC: serous carcinoma; NA: not applicable. *Statistically significant.

Table VI. *Differences in progression-free survival among histological types.*

Histological type	*p*-Value					
	Grade 1 EC	Grade 2 EC	Grade 3 EC	CS	SC	MLA
Grade 1 EC	–	0.207	<0.001*	<0.001*	<0.001*	<0.001*
Grade 2 EC	0.207	–	0.012*	<0.001*	<0.001*	<0.001*
Grade 3 EC	<0.001*	0.012*	–	0.010*	<0.001*	<0.001*
CS	<0.001*	<0.001*	0.010*	–	0.662	0.263
SC	<0.001*	<0.001*	<0.001*	0.662	–	0.343
MLA	<0.001*	<0.001*	<0.001*	0.263	0.343	–

CS: Carcinosarcoma; EC: endometrioid carcinoma; MLA: mesonephric-like adenocarcinoma; SC: serous carcinoma. *Statistically significant.

in our series (7/237; 3.0%) was higher than that (4/570; 0.7%) of a recent retrospective study by Kolin *et al*. (33), who identified uterine MLA cases according to the following morphological and molecular features: typical histological features, *KRAS* mutation, absence of microsatellite instability, and lack of squamous or mucinous differentiation, and reported that *KRAS*-mutated, microsatellite-stable endometrial carcinomas lacking squamous or mucinous differentiation are more likely to be MLAs. The higher prevalence of uterine MLAs in our case series could be due to under-recognition as identifying uterine MLA has only recently been described in the literature, and the condition morphologically overlaps with EC, SC, and CS to some degree.

Figure 5 summarizes the clinicopathological, immunophenotypical, and genetic characteristics of uterine MLA cases in our study. More than half (4/7) of the uterine MLA patients were diagnosed with advanced-stage disease. All (7/7) cases showed deep myometrial invasion and LVSI, and more than half (4/7) of the patients developed metastases within eight months of surgery. All (3/3) patients with early-stage tumors experienced local recurrences and metastases 14 months post-operation. The lungs were the most common metastatic site, as five patients developed pulmonary metastases either synchronously or metachronously. Several previous studies have also reported high frequencies of lung metastases in patients with uterine MLA (1, 9, 15, 33, 34). Optimal management of cases of uterine MLA mandates careful surveillance for recurrence and metastasis after a potentially curative resection. Since rapid progression was common even for early-stage disease, intensive monitoring of all uterine MLA patients should be undertaken during the postoperative period for the early detection of recurrence and metastasis.

GATA3 has been known to be the most sensitive and specific marker for mesonephric lesions (13). In this study, at least moderate GATA3 positivity was observed in all cases except one. GATA3 staining intensity was strong even in patchy areas. Solid areas displayed reduced GATA3 expression compared to tubular and papillary areas, consistent with previous reports (1, 13, 14). Although the sensitivity and specificity of GATA3 in the cervical mesonephric lesions are as high as 90%, they are lower in the mesonephric lesions arising in the adnexa (13). Previous studies have shown that a small subset of premalignant and malignant endometrial lesions expressed GATA3, including atypical hyperplasia, EC, SC, and CS, with variable staining intensity and proportion (35, 36). Furthermore, a recent study suggested that GATA3 immunostaining should not be used to distinguish between mesonephric-like CS and conventional CS because GATA3 also reacts with a substantial number of conventional CS tumor cells (14). Therefore, positive immunoreactivities for other mesonephric markers, including PAX2, TTF1, and CD10 can be helpful in GATA3-negative cases (9, 10, 14). In our case series, all MLAs showed nuclear PAX2 immunoreactivity in at least 50% of tumor cells. TTF1 and CD10 were also positive in most of the MLA cases with at least moderate staining intensity. One case showed complete absence of GATA3 and TTF1, but immunoreactivity analysis reported the case as MLA because PAX2 and CD10 were diffusely and strongly positive in the tumor cell nuclei and along the luminal surface of tubules and ducts, respectively. Taken together, variable staining intensities and proportions of GATA3, CD10, and TTF1 in cells may pose challenges in the diagnosis of uterine MLA. When interpreting immunostained slides, pathologists should consider that immunostaining results may not always be straightforward. Immunostaining for a combination of more than one factors should be advantageous in unusual settings where a suspicious case displays negative staining for one or two mesonephric markers.

ER expression is typically absent in cases of uterine MLA. However, focal ER positivity has been observed in some MLA cases, with weak-to-moderate intensity (2, 9). PR is also known to be negative in most MLA cases, but a few have shown focal or patchy PR positivity (2, 9). In this study, one case exhibited patchy and weak-to-moderate ER immunoreactivity in 10% of the tumor cells, while PR was negative in all examined cases. Thus, immunostaining for

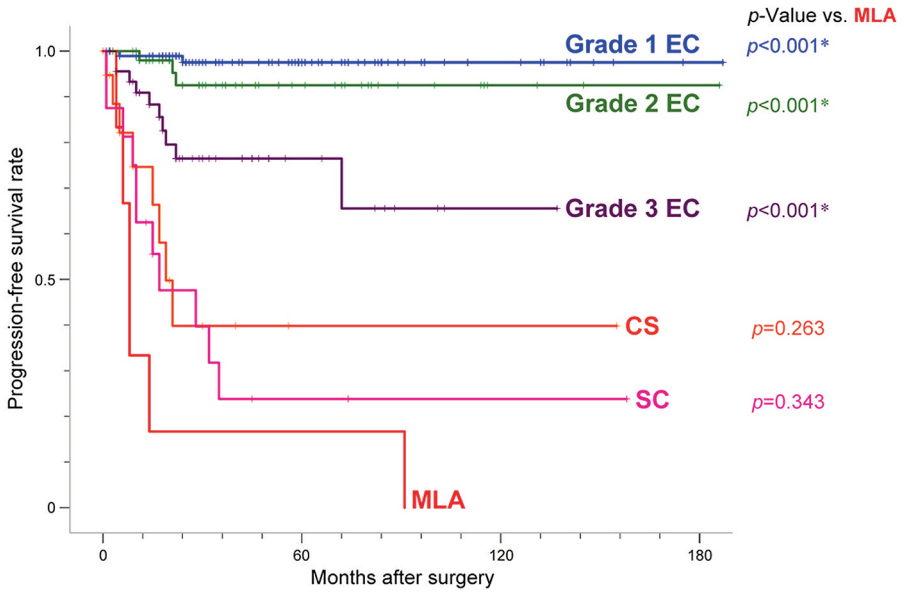


Figure 4. *Differences in progression-free survival (PFS) among uterine mesonephric-like adenocarcinoma (MLA) and other histological types of endometrial carcinoma, including endometrioid carcinoma (EC), carcinosarcoma (CS), and serous carcinoma (SC). All MLA patients developed post-operative recurrences. PFS of MLA was significantly worse than that of grade 1, 2, and 3 EC. Patients with MLA also had a lower PFS rate than those with CS and SC, but the differences were not significant.*

hormone receptors may assist pathologists confirm the diagnosis of MLA when performed in addition to the mesonephric markers. Further, the non-diffuse p16 positivity and wild-type p53 immunostaining pattern help exclude cases of SC, except for rare cases that harbor pathogenic *TP53* mutations without aberrant p53 staining.

NGS analysis revealed that all except one MLA harbored activating *KRAS* mutations [G12D (3/6), G12V (2/6), and G12D (1/6)]. Frequent *KRAS* mutations in MLA have been documented consistently in previous studies (1, 8, 9, 15). The identification of *ARID1A* mutation in two of the cases in the present study was in line with previous observations of *ARID1A* and *PIK3CA* co-alterations in MLA (8, 9). Although recurrent *KRAS* and *ARID1A* mutations have been detected, mutations of both the genes are not specific for MLA. It is well known that a considerable proportion of EC cases harbor pathogenic mutations in *ARID1A* and *KRAS* (9, 33).

Moreover, we also found that one MLA case harbored a pathogenic frameshift *ATM* mutation (c.8395_8404del; p.F2799fs), causing a truncation of the encoded protein. There have been two reported cases of malignant mesonephric lesions harboring *ATM* mutations (37, 38). Marani *et al.* (37) presented a case of cervical mesonephric carcinosarcoma showing a missense *ATM* mutation (c.2572T>C; p.F858L) with conflicting interpretations of pathogenicity. Seay *et al.* (38) detected a variant of uncertain significance in the *ATM* gene (c.4303A>C; p.K1435Q) in a case of ovarian MLA. To the best of our knowledge, the present study is the first to identify a truncating *ATM* mutation in MLA, which caused loss of function of the ATM protein.

We investigated the differences in various clinico-pathological features among histological types. Several features of MLA were significantly different from those of EC, SC, or CS. MLA patients were older than those with EC; the tumor size in MLA was larger than that in EC; deep myometrial invasion, LVSI, FIGO stage III-IV disease, and coagulative tumor cell necrosis were more frequently identified in MLA than in EC. The following histological features were observed in all MLA cases: overlapping nuclei, angulated nuclei, scant cytoplasm, more than three architectural patterns, compactly aggregated small tubules, and eosinophilic intraluminal secretions. The frequencies of the last four features were significantly higher in MLA than those in EC, SC, and CS. Spindle cells were also more frequently observed in MLA than in EC and SC. In contrast, severe nuclear pleomorphism was more frequently observed in SC and CS than in MLA, as the latter typically possessed low-to-intermediate-grade nuclei. The frequency of prominent nucleoli in MLA (14.3%) was significantly lower than that in EC, SC, and CS, all of which possessed prominent nucleoli in more than half (63.6%, 92.3%, and 100.0%, respectively) of all cases. Mitotic activity of MLA was higher than that of EC, but lower than those of SC and CS. Squamous or mucinous differentiation was observed in EC and CS, but not in MLA and SC. Overall, histological features

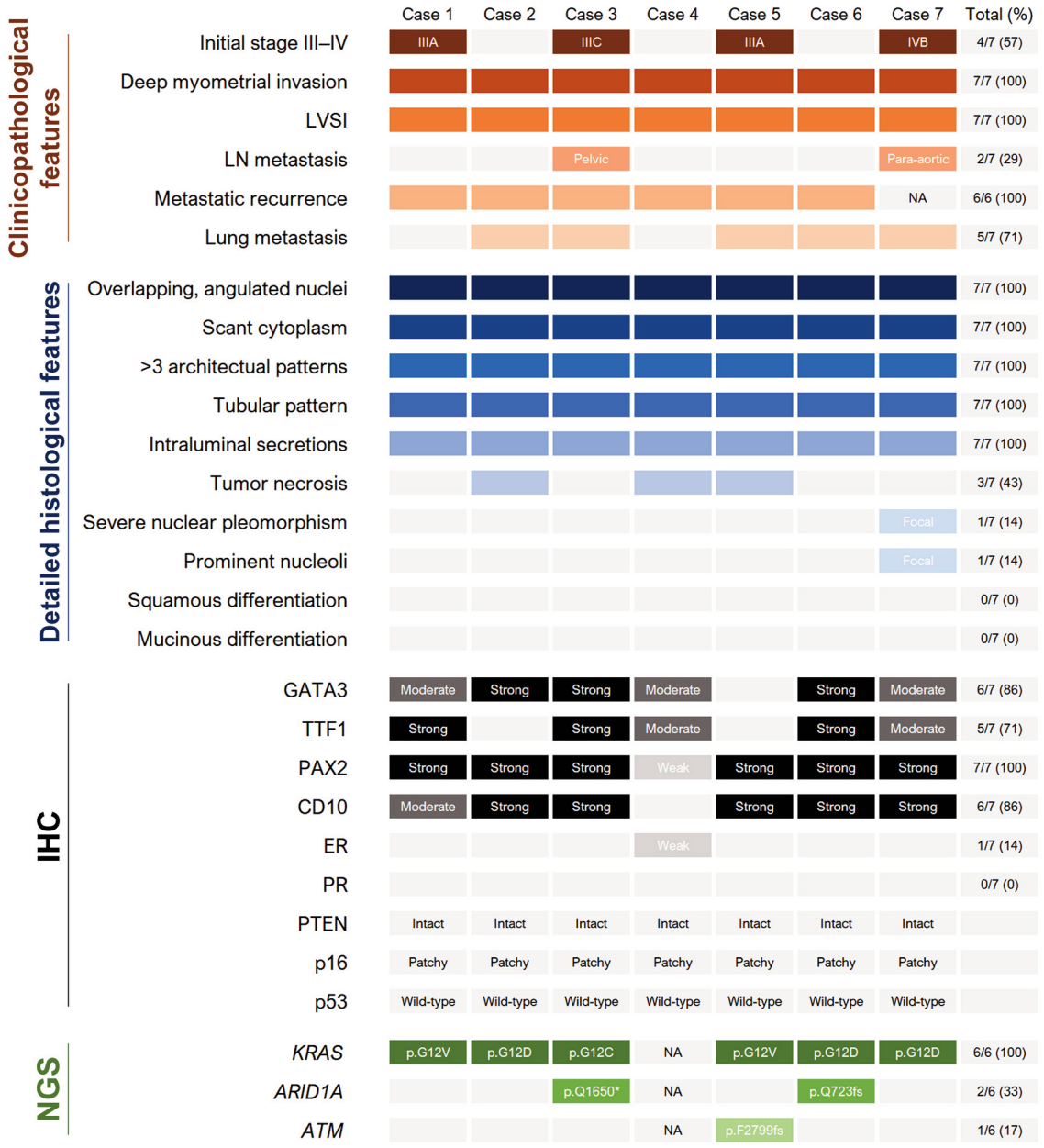


Figure 5. *Summary of clinicopathological and molecular characteristics of uterine MLA. MLA: Mesonephric-like adenocarcinoma; ATM: ataxia telangiectasia mutated; ARID1A: AT-rich interaction domain; CD10: cluster of differentiation 10; ER: estrogen receptor; GATA3: GATA-binding protein 3; IHC: immunohistochemistry; KRAS: Kirsten rat sarcoma viral oncogene homolog; LN: lymph node; LVSI: lymphovascular space invasion; NA: not applicable; NGS: next-generation sequencing; PAX2: paired box 2; PR: progesterone receptor; TTF1: transcription termination factor 1.*

favoring MLA included hyperchromatic nuclei with overlapping and angulation, scant cytoplasm, inconspicuous nucleoli, architectural diversity with more than three patterns, tubular pattern, spindle cells, eosinophilic intraluminal secretions, and absence of squamous or mucinous differentiation. However, these features are not specific for MLA. High-grade EC can show relatively small, hyperchromatic nuclei, and scant cytoplasm, resulting in high nuclear-to-cytoplasmic ratio. We recently demonstrated that low-grade EC with mesonephric-like differentiation (EC-MLD) exhibits various growth patterns, including solid, papillary, villoglandular, sex cord-like, and even tubular patterns. All EC-MLD cases possessed eosinophilic

intraluminal secretions. Moreover, we observed a case of serous carcinoma with mesonephric-like differentiation that was initially misdiagnosed as MLA. This unusual tumor showed easily identifiable intraluminal eosinophilic substances within the tubules and glands, but they were not as dense as those typically observed in mesonephric lesions. SC has irregular, shattered intraglandular materials that are not the same shape as the lumen, whereas MLA has deeply eosinophilic, hyaline-like secretions, which are typically stained bright pink by hematoxylin and eosin and similar to those observed in benign mesonephric lesions or thyroid follicles. The intraluminal secretions of MLA usually conform to the contours of the glands in which they are found. Since the cytoplasm amount, nuclear shape, architectural diversity, and nature of intraluminal secretions are neither specific nor pathognomonic in MLA, ancillary tests including immunostaining and targeted sequencing analysis are recommended for an accurate diagnosis.

If pathologists are unaware of this peculiarity, they can misdiagnose uterine MLA as endometrial EC, especially when only a small amount of endometrial tissue is obtained by biopsy or curettage. An admixture of well-formed, endometrioid-like ducts and glands and thin papillae in an endometrial curettage specimen can be misinterpreted as low-grade endometrial EC. The possibility of uterine MLA should be reported if the following histological features are noted: deeply basophilic appearance at scanning or low-power magnification due to compact aggregation of small tubules with hyperchromatic, angulated, and overlapped nuclei, scant cytoplasm, and high nuclear-to-cytoplasmic ratio; merging of several architectural patterns; and eosinophilic, hyaline-like intraluminal secretions. Immunostaining with a panel of antibodies, including those for mesonephric markers and hormone receptors can help obtain an accurate diagnosis. When immunostaining reveals conflicting results, a differential diagnosis should be conducted. A description of relevant histological findings should be written, with a comment explaining the diagnostic possibility of MLA.

Figure 4 demonstrates the survival data of patients with MLA, EC, SC, and CS. The PFS of grade 3 EC was significantly shorter than that of grade 1-2 EC. SC, CS, and MLA had a significantly shorter PFS than grade 3 EC. MLA showed a lower PFS rate than CS and SC, but the differences were not significant. In general, severe nuclear atypia, including enlargement, pleomorphism, and conspicuous nucleoli, reflects oncogenic aggressiveness and poor prognosis of high-grade endometrial carcinoma. In this study; however, even though all except one MLA case exhibited relatively small nuclei with minimal-to-mild pleomorphism and inconspicuous nucleoli, the PFS rate of MLA was lower than that of any other histological type. In agreement with our previous data (1), the degree of nuclear atypia did not show a significant relationship with the aggressive biological behavior of MLA. Our observations suggest that the conventional grading system may not appropriately reflect the severity of uterine MLA. Unfortunately, there is no standard histological grading system for nuclear atypia of MLA. Further investigations are warranted to establish reliable guidelines to assist pathologists in determining the degree of nuclear atypia.

Several previous studies have compared the survival rate of patients with MLA with that of those with other histological types of endometrial carcinoma. Euscher *et al*. (9) demonstrated significant differences in survival among low-grade endometrial EC, endometrial SC, and uterine MLA. They observed a substantial difference in both PFS and overall survival (OS) between these three groups, with MLA showing a shorter PFS and lower OS than those of low-grade EC and SC. In a recent multi-center study by Pors *et al*. (14), the PFS of MLA was compared with those of other endometrial carcinoma types using The Cancer Genome Atlas database. MLA had worse PFS than EC, but it was not significantly different from that of SC or CS. Our results are consistent with those of these previous studies. These data indicate that MLA patients experience earlier recurrences and distant metastases similar to or more frequently than SC and CS patients, but the mortality rate of MLA is not significantly different. Even though uterine MLAs are a clinically aggressive group of gynecologic carcinomas, they can be considered to have a long clinical course. Additional studies with larger sample sizes and longer follow-up periods are necessary.

In summary, MLA of the uterine corpus is a rare but clinicopathologically distinct histological type of gynecological malignancy with several characteristic histological features, such as multiple and merging growth patterns, including compactly aggregated small tubules; eosinophilic intraluminal secretions; and cells with relatively small, angulated, overlapping nuclei, and scant cytoplasm. Immunohistochemically, the expression of one or more mesonephric markers (GATA-3, TTF-1, CD10, or PAX2) and the absence or marked reduction in the expression of hormone receptors facilitate its diagnosis. The majority of uterine MLAs harbor *KRAS* mutations. The present study was the first to identify a pathogenic truncating *ATM* mutation in one of our uterine MLA cases. We observed that uterine MLA behaves more aggressively than the more commonly encountered types of endometrial carcinoma, with larger tumor size, deeper myometrial invasion, more advanced-stage disease, and more frequent LVSI. All patients developed post-operative metastases, with a striking predilection to the lungs, and had the lowest PFS rate compared to all other types of endometrial carcinoma.

Conflicts of Interest

None of the Authors have any conflicts of interest or financial ties to declare regarding this study.

Authors' Contributions

All Authors made substantial contributions to the conceptualization and design of the study; acquisition, analysis, interpretation, and validation of data; drafting of the manuscript; critical revision of the manuscript to highlight important content; and final approval of the version for publishing.

Acknowledgements

This research was supported by the Basic Science Research Program through the National Research Foundation of Korea (NRF) funded by the Ministry of Science, ICT, and Future Planning (2020R1G1A1003692), the Bio and Medical Technology Development Program of the NRF funded by the Korean government (MSIT) (2019M3E5D1A02068558), and a grant of the Korea health Technology R&D Project through the Korea Health Industry Development Institute (KHIDI) funded by Ministry of Health & Welfare, Republic of Korea (HR20C0025).

References

1 Na K and Kim HS: Clinicopathologic and molecular characteristics of mesonephric adenocarcinoma arising from the uterine body. Am J Surg Pathol *43(1)*: 12-25, 2019. PMID: 29189288. DOI: 10.1097/PAS.0000000000000991

2 Kim H, Na K, Bae GE and Kim HS: Mesonephric-like adenocarcinoma of the uterine corpus: Comprehensive immunohistochemical analyses using markers for mesonephric, endometrioid and serous tumors. Diagnostics (Basel) *11(11)*: 2042, 2021. PMID: 34829389. DOI: 10.3390/diagnostics11112042

3 Lee H, Kim H and Kim HS: Mesonephric adenocarcinoma of the vagina harboring *TP53* mutation. Diagnostics (Basel) *12(1)*: 119, 2022. PMID: 35054285. DOI: 10.3390/diagnostics12010119

4 Howitt BE and Nucci MR: Mesonephric proliferations of the female genital tract. Pathology *50(2)*: 141-150, 2018. PMID: 29269124. DOI: 10.1016/j.pathol.2017.11.084

5 Koh HH, Park E and Kim HS: Mesonephric-like adenocarcinoma of the ovary: clinicopathological and molecular characteristics. Diagnostics (Basel) *12(2)*: 326, 2022. PMID: 35204416. DOI: 10.3390/diagnostics12020326

6 McFarland M, Quick CM and McCluggage WG: Hormone receptor-negative, thyroid transcription factor 1-positive uterine and ovarian adenocarcinomas: report of a series of mesonephric-like adenocarcinomas. Histopathology *68(7)*: 1013-1020, 2016. PMID: 26484981. DOI: 10.1111/his.12895

7 Roma AA: Mesonephric carcinosarcoma involving uterine cervix and vagina: report of 2 cases with immunohistochemical positivity For PAX2, PAX8, and GATA-3. Int J Gynecol Pathol *33(6)*: 624-629, 2014. PMID: 25272303. DOI: 10.1097/PGP.0000000000000088

8 Lin DI, Shah N, Tse JY, Killian JK, Hemmerich A, Edgerly C, Haberberger J, Severson EA, Huang RSP, Ramkissoon SH, Vergilio JA, Ross JS and Elvin JA: Molecular profiling of mesonephric and mesonephric-like carcinomas of cervical, endometrial and ovarian origin. Gynecol Oncol Rep *34*: 100652, 2020. PMID: 33024807. DOI: 10.1016/j.gore.2020.100652

9 Euscher ED, Bassett R, Duose DY, Lan C, Wistuba I, Ramondetta L, Ramalingam P and Malpica A: Mesonephric-like carcinoma of the endometrium: a subset of endometrial carcinoma with an aggressive behavior. Am J Surg Pathol *44(4)*: 429-443, 2020. PMID: 31725471. DOI: 10.1097/PAS.0000000000001401

10 Horn LC, Höhn AK, Krücken I, Stiller M, Obeck U and Brambs CE: Mesonephric-like adenocarcinomas of the uterine corpus: report of a case series and review of the literature indicating poor prognosis for this subtype of endometrial adenocarcinoma. J Cancer Res Clin Oncol *146(4)*: 971-983, 2020. PMID: 31927619. DOI: 10.1007/s00432-019-03123-7

11 Deolet E, Van Dorpe J and Van de Vijver K: Mesonephric-like adenocarcinoma of the endometrium: diagnostic advances to spot this wolf in sheep's clothing. A review of the literature. J Clin Med *10(4)*: 698, 2021. PMID: 33670088. DOI: 10.3390/jcm10040698

12 Mirkovic J, Sholl LM, Garcia E, Lindeman N, MacConaill L, Hirsch M, Dal Cin P, Gorman M, Barletta JA, Nucci MR, McCluggage WG and Howitt BE: Targeted genomic profiling reveals recurrent *KRAS* mutations and gain of chromosome 1q in mesonephric carcinomas of the female genital tract. Mod Pathol *28(11)*: 1504-1514, 2015. PMID: 26336887. DOI: 10.1038/modpathol.2015.103

13 Howitt BE, Emori MM, Drapkin R, Gaspar C, Barletta JA, Nucci MR, McCluggage WG, Oliva E and Hirsch MS: GATA3 is a sensitive and specific marker of benign and malignant mesonephric lesions in the lower female genital tract. Am J Surg Pathol *39(10)*: 1411-1419, 2015. PMID: 26135559. DOI: 10.1097/PAS.0000000000000471

14 Pors J, Cheng A, Leo JM, Kinloch MA, Gilks B and Hoang L: A comparison of GATA3, TTF1, CD10, and calretinin in identifying mesonephric and mesonephric-like carcinomas of the gynecologic tract. Am J Surg Pathol *42(12)*: 1596-1606, 2018. PMID: 30148742. DOI: 10.1097/PAS.0000000000001142

15 Mirkovic J, McFarland M, Garcia E, Sholl LM, Lindeman N, MacConaill L, Dong F, Hirsch M, Nucci MR, Quick CM, Crum CP, McCluggage WG and Howitt BE: Targeted genomic profiling reveals recurrent *KRAS* mutations in mesonephric-like adenocarcinomas of the female genital tract. Am J Surg Pathol *42(2)*: 227-233, 2018. PMID: 28984674. DOI: 10.1097/PAS.0000000000000958

16 Park S, Bae GE, Kim J and Kim HS: Mesonephric-like differentiation of endometrial endometrioid carcinoma: Clinicopathological and molecular characteristics distinct from those of uterine mesonephric-like adenocarcinoma. Diagnostics (Basel) *11(8)*: 1450, 2021. PMID: 34441384. DOI: 10.3390/diagnostics11081450

17 Na K and Kim HS: Clinicopathological characteristics of fallopian tube metastases from primary endometrial, cervical, and nongynecological malignancies: a single institutional experience. Virchows Arch *471(3)*: 363-373, 2017. PMID: 28702779. DOI: 10.1007/s00428-017-2186-z

18 Kim SW, Park BJ, Kim HS and Na K: Diagnostic utility of oncomine comprehensive assay v3 in differentiating between isocitrate dehydrogenase (IDH)-mutated grade II-III astrocytoma and oligodendroglioma. In Vivo *35(2)*: 921-927, 2021. PMID: 33622884. DOI: 10.21873/invivo.12332

19 Jung YY, Woo HY and Kim HS: Targeted genomic sequencing reveals novel *TP53* in-frame deletion mutations leading to p53 overexpression in high-grade serous tubo-ovarian carcinoma. Anticancer Res *39(6)*: 2883-2889, 2019. PMID: 31177126. DOI: 10.21873/anticanres.13417

20 Choi S, Na K, Kim SW and Kim HS: Dedifferentiated mesonephric-like adenocarcinoma of the uterine corpus. Anticancer Res *41(5)*: 2719-2726, 2021. PMID: 33952503. DOI: 10.21873/anticanres.15053

21 Choi S, Park S, Chung MP, Kim TS, Cho JH and Han J: A rare case of adenosquamous carcinoma arising in the background of IgG4-related lung disease. J Pathol Transl Med *53(3)*: 188-191, 2019. PMID: 30853707. DOI: 10.4132/jptm.2019.02.21

22 Jang Y, Jung H, Kim HN, Seo Y, Alsharif E, Nam SJ, Kim SW, Lee JE, Park YH, Cho EY and Cho SY: Clinicopathologic characteristics of HER2-positive pure mucinous carcinoma of the breast. J Pathol Transl Med *54(1)*: 95-102, 2020. PMID: 31718120. DOI: 10.4132/jptm.2019.10.24

23 Kim H, Kim J, Lee SK, Cho EY and Cho SY: TFE3-expressing perivascular epithelioid cell tumor of the breast. J Pathol Transl Med *53(1)*: 62-65, 2019. PMID: 30269476. DOI: 10.4132/jptm.2018.08.30

24 Choi S, Cho J, Lee SE, Baek CH, Kim YK, Kim HJ and Ko YH: Adenocarcinoma of the minor salivary gland with concurrent MAML2 and EWSR1 alterations. J Pathol Transl Med *55(2)*: 132-138, 2021. PMID: 33472334. DOI: 10.4132/jptm.2020.12.11

25 Kim H, Yoon N, Woo HY, Lee EJ, DO SI, Na K and Kim HS: Atypical mesonephric hyperplasia of the uterus harbors pathogenic mutation of Kirsten rat sarcoma 2 viral oncogene homolog (*KRAS*) and gain of chromosome 1q. Cancer Genomics Proteomics *17(6)*: 813-826, 2020. PMID: 33099482. DOI: 10.21873/cgp.20235

26 Choi KH, Kim H, Bae GE, Lee SH, Woo HY and Kim HS: Mesonephric-like differentiation of ovarian endometrioid and high-grade serous carcinomas: Clinicopathological and molecular characteristics distinct from those of mesonephric-like adenocarcinoma. Anticancer Res *41(9)*: 4587-4601, 2021. PMID: 34475087. DOI: 10.21873/anticanres.15272

27 Kwon HJ, Song SY and Kim HS: Prominent papillary growth pattern and severe nuclear pleomorphism induced by neoadjuvant chemotherapy in ovarian mucinous carcinoma: potential for misdiagnosis as high-grade serous carcinoma. Anticancer Res *41(3)*: 1579-1586, 2021. PMID: 33788752. DOI: 10.21873/anticanres.14918

28 Köbel M, Ronnett BM, Singh N, Soslow RA, Gilks CB and McCluggage WG: Interpretation of p53 immunohistochemistry in endometrial carcinomas: toward increased reproducibility. Int J Gynecol Pathol *38(Suppl 1)*: S123-S131, 2019. PMID: 29517499. DOI: 10.1097/PGP.0000000000000488

29 Chung T, DO SI, Na K, Kim G, Jeong YI, Kim YW and Kim HS: Stromal p16 overexpression in gastric-type mucinous carcinoma of the uterine cervix. Anticancer Res *38(6)*: 3551-3558, 2018. PMID: 29848709. DOI: 10.21873/anticanres.12627

30 Na K, Sung JY and Kim HS: Clinicopathological characteristics of high-grade squamous intraepithelial lesions involving condyloma acuminatum. Anticancer Res *38(3)*: 1767-1774, 2018. PMID: 29491115. DOI: 10.21873/anticanres.12414

31 Jung YY, Nahm JH and Kim HS: Cytomorphological characteristics of glassy cell carcinoma of the uterine cervix: histopathological correlation and human papillomavirus genotyping. Oncotarget *7(45)*: 74152-74161, 2016. PMID: 27708230. DOI: 10.18632/oncotarget.12361

32 Woo HY, Na K, Yoo J, Chang JH, Park YN, Shim HS and Kim SH: Glioblastomas harboring gene fusions detected by next-generation sequencing. Brain Tumor Pathol *37(4)*: 136-144, 2020. PMID: 32761533. DOI: 10.1007/s10014-020-00377-9

33 Kolin DL, Costigan DC, Dong F, Nucci MR and Howitt BE: A combined morphologic and molecular approach to retrospectively identify *KRAS*-mutated mesonephric-like adenocarcinomas of the endometrium. Am J Surg Pathol *43(3)*: 389-398, 2019. PMID: 30489318. DOI: 10.1097/PAS.0000000000001193

34 Yamamoto S and Sakai Y: Pulmonary metastasis of mesonephric-like adenocarcinoma arising from the uterine body: a striking mimic of follicular thyroid carcinoma. Histopathology *74(4)*: 651-653, 2019. PMID: 30471132. DOI: 10.1111/his.13798

35 Terzic T, Mills AM, Zadeh S, Atkins KA and Hanley KZ: GATA3 expression in common gynecologic carcinomas: a potential pitfall. Int J Gynecol Pathol *38(5)*: 485-492, 2019. PMID: 30059453. DOI: 10.1097/PGP.0000000000000541

36 Roma AA, Goyal A and Yang B: Differential expression patterns of GATA3 in uterine mesonephric and nonmesonephric lesions. Int J Gynecol Pathol *34(5)*: 480-486, 2015. PMID: 25851711. DOI: 10.1097/PGP.0000000000000167

37 Marani C, Akaev I, Yeoh CC, Walsh E and Rahimi S: Cervical malignant mixed mesonephric tumour: A case report with local recurrence after six-years and next-generation sequencing analysis with particular reference to the ataxia telangiectasia mutated gene. Exp Ther Med *21(4)*: 394, 2021. PMID: 33680116. DOI: 10.3892/etm.2021.9825

38 Seay K, Akanbi T, Bustamante B, Chaudhary S and Goldberg GL: Mesonephric-like adenocarcinoma of the ovary with co-existent endometriosis: A case report and review of the literature. Gynecol Oncol Rep *34*: 100657, 2020. PMID: 33088886. DOI: 10.1016/j.gore.2020.100657

Received March 14, 2022
Revised April 13, 2022
Accepted April 14, 2022